THE JOURNAL OF BIOLOGICAL CHEMISTRY VOL. 291, NO. 19, pp. 10032–10045, May 6, 2016

Activation of Vascular Endothelial Growth Factor (VEGF) Receptor 2 Mediates Endothelial Permeability Caused by Cyclic Stretch*

Received for publication, September 4, 2015, and in revised form, February 3, 2016 Published, JBC Papers in Press, February 16, 2016, DOI 10.1074/jbc.M115.690487

Yufeng Tian, Grzegorz Gawlak, James J. O'Donnell III, Anna A. Birukova, and Konstantin G. Birukov[1]

From the Lung Injury Center and Section of Pulmonary and Critical Care Medicine, Department of Medicine, University of Chicago, Chicago, Illinois 60637

High tidal volume mechanical ventilation and the resultant excessive mechanical forces experienced by lung vascular endothelium are known to lead to increased vascular endothelial leak, but the underlying molecular mechanisms remain incompletely understood. One reported mechanotransduction pathway of increased endothelial cell (EC) permeability caused by high magnitude cyclic stretch (18% CS) involves CS-induced activation of the focal adhesion associated signalosome, which triggers Rho GTPase signaling. This study identified an alternative pathway of CS-induced EC permeability. We show here that high magnitude cyclic stretch (18% CS) rapidly activates VEGF receptor 2 (VEGFR2) signaling by dissociating VEGFR2 from VE-cadherin at the cell junctions. This results in VEGFR2 activation, Src-dependent VE-cadherin tyrosine phosphorylation, and internalization leading to increased endothelial permeability. This process is also accompanied by CS-induced phosphorylation and internalization of PECAM1. Importantly, CS-induced endothelial barrier disruption was attenuated by VEGFR2 inhibition. 18% CS-induced EC permeability was linked to dissociation of cell junction scaffold afadin from the adherens junctions. Forced expression of recombinant afadin in pulmonary endothelium attenuated CS-induced VEGFR2 and VE-cadherin phosphorylation, preserved adherens junction integrity and VEGFR2·VE-cadherin complex, and suppressed CS-induced EC permeability. This study shows for the first time a mechanism whereby VEGFR2 activation mediates EC permeability induced by pathologically relevant cyclic stretch. In this mechanism, CS induces dissociation of the VE-cadherin·VEGFR2 complex localized at the adherens juctions, causing activation of VEGFR2, VEGFR2-mediated Src-dependent phosphorylation of VE-cadherin, disassembly of adherens junctions, and EC barrier failure.

Ventilator support is an indispensable treatment for critically ill patients. However, difficulties with precise evaluation of functional ventilated lung volumes in patients with inflamed lungs lead to a suboptimal regimen of mechanical ventilation, culminating in ventilator-induced lung injury and multiorgan dysfunction. As a result, high rates of morbidity and mortality remain one of the most important problems in the management of patients with pre-existing respiratory complications in the intensive care unit (1, 2). Increased lung vascular leakiness caused by mechanical ventilation at elevated tidal volumes is a major contributor to alveolar flooding and pulmonary edema.

Endothelial cell (EC)[2] junctions called adherens junctions (AJ) play a key role in the regulation of vascular endothelial permeability (3–6). VE-cadherin promotes homophilic adhesion in vascular endothelium, forming zipper-like AJs along cell contacts. Cytoplasmic and transmembrane VE-cadherin domains interact with intracellular partners, including regulatory protein p120-catenin, α,β,γ-catenins that link VE-cadherin with cytoskeleton, signaling kinases, and receptors (7–10). Afadin is another important AJ-associated protein, controlling assembly of cell-cell junctions in epithelial and endothelial monolayers (11, 12). Afadin also mediates agonist-induced assembly of AJ complexes, as well as physical interactions between adherens junctions and tight junctions, which contribute to agonist-induced EC barrier enhancement (13, 14).

In addition to playing a key structural role in formation of AJ complexes that maintain the integrity of endothelial monolayer in the lung, VE-cadherin participates in autoregulation of AJ assembly by coordinating local signaling. Mechanisms by which VE-cadherin can transduce intracellular signals include binding to VEGF receptor 2 (VEGFR2), which prevents VEGFR2 phosphorylation, internalization, and signaling to MAPK; binding to and assembly of TGF-β receptor complex, which enhances Smad-dependent transcription; and signaling through small GTPases including Rho/ROCK to promote actomyosin contraction, Rac1/Tiam1, and Rap1/Epac (15).

Studies of flow-induced mechanotransduction in vascular endothelium revealed a novel role of VE-cadherin as part of mechanosensitive complex containing VE-cadherin, PECAM1, and VEGFR2 (16). This complex coordinates flow-induced cell reorientation and activation of cell substrate adhesive complexes. Moreover, VEGFR2 phosphorylation plays important role in flow-induced inflammatory activation of vascular endo-

* This work was supported by NHLBI, National Institutes of Health Grants HL87823, HL076259, HL107920, and GM114171. The authors declare that they have no conflicts of interest with the contents of this article. The content is solely the responsibility of the authors and does not necessarily represent the official views of the National Institutes of Health.

[1] To whom correspondence should be addressed: Lung Injury Center, Section of Pulmonary and Critical Medicine, Dept. of Medicine, University of Chicago, 5841 S. Maryland Ave., Office N-611, Chicago, IL 60637. Tel.: 773-834-2636; Fax: 773-834-2683; E-mail: kbirukov@medicine.bsd.uchicago.edu.

[2] The abbreviations used are: EC, endothelial cell; VEGFR, VEGF receptor; CS, cyclic stretch; AJ, adherens junction; HPAEC, human pulmonary artery endothelial cell; ns-RNA, non-specific RNA.

thelium exposed to disturbed flow (16). Physical association of VE-cadherin and VEGFR2 at AJ suppresses VEGFR2-mediated signaling and thus limits EC permeability. On the other hand, dissociation of VEGFR2·VE-cadherin complex promotes VEGFR2 autophosphorylation and activation (17). Interestingly, VEGFR2 transactivation has been observed in another case of AJ disruption caused by truncated phospholipids. In those conditions, acute barrier dysfunction was associated with rapid internalization of VE-cadherin and stimulation of VEGFR2 tyrosine phosphorylation, which caused a delayed activation of the VEGFR2-RhoA pathway of EC permeability (18). Taken together, these findings emphasize the importance of VEGFR2/VE-cadherin association for the maintenance of EC barrier under flow conditions.

Potential involvement of AJ-associated signaling in the EC dysfunction caused by pathologically relevant high magnitude cyclic stretch remains unknown. Cell models recapitulating ventilation-associated mechanical strain experienced by lung vascular endothelium and epithelium have been developed by our and other groups (19–24). Exposure of pulmonary EC monolayers to pathologically relevant high magnitude CS exacerbated EC permeability caused by vasoactive and proinflammatory mediators by enhancing agonist-induced activation of RhoA pathway of EC barrier dysfunction (20, 25–27). CS also may directly activate Rho signaling via stretch-induced assembly of focal adhesion-associated signaling complex containing paxillin, MAP kinase, and Rho-specific nucleotide exchange factor GEF-H1. These events trigger GEF-H1-RhoA-mediated pathway of EC permeability (28). Whether the VE-cadherin·VEGFR2 complex can be affected by elevated CS amplitudes and whether this mechanism contributes to the sustained vascular leak in lung vasculature under excessive mechanical strain remain unknown. This mechanism was tested in this study.

Experimental Procedures

Reagents and Cell Culture—Human thrombin was obtained from Sigma. VEGFR2 inhibitor SU-1498, Src kinase family inhibitor PP2, and phosphotyrosine (4G10) antibody was obtained from EMD Millipore (Billerica, MA). VE-cadherin, p120-catenin, afadin, and EEA1 antibodies were obtained from BD Transduction Laboratories (San Diego, CA); PECAM1 and Na^+/K^+-ATPase antibodies were from Santa Cruz Biotechnology (Santa Cruz, CA); BV9 antibody interacting with VE-cadherin extracellular domain and mouse monoclonal GFP antibody were obtained from Abcam (Cambridge, MA); phospho-VEGFR2, MEK1/2, and HRP-linked anti-mouse and anti-rabbit IgG antibodies were obtained from Cell Signaling (Beverly, MA). Texas Red phalloidin- and Alexa Flour 488-conjugated secondary antibodies were purchased form Molecular Probes (Eugene, OR). Unless otherwise specified, biochemical reagents were obtained from Sigma. Human pulmonary artery endothelial cells (HPAEC) were obtained from Lonza (Allendale, NJ), cultured according to the manufacturer's protocol, and used at passages 5–7. Apoptosis assay was performed using a viability/cytotoxicity kit from Molecular Probes according to the manufacturer's protocol.

DNA and siRNA Transfections—Sets of VEGFR2- and afadin-specific oligonucleotides (Stealth Select) were obtained from Invitrogen and characterized previously (18, 29). Transfection of EC with siRNA was performed as previously described (20, 30). After 48–72 h of transfection, cells were used for experiments or harvested for Western blot verification of specific protein depletion. Plasmid encoding wild type afadin bearing EGFP tag was kindly provided by Y. Takai (Kobe University, Kobe, Japan). EC were used for transient transfections according to protocol described previously (31).

Cell Culture under Cyclic Stretch—All cyclic stretch experiments were performed using FX-4000T Flexcell Tension Plus system (Flexcell International, McKeesport, PA) equipped with a 25-mm BioFlex Loading station, as previously described (26, 32). The experiments were performed in the presence of culture medium containing 2% fetal bovine serum. HPAEC were seeded at standard densities (8×10^5 cells/well) onto collagen I-coated flexible bottom BioFlex plates. EC were exposed to CS at 18% distension, sinusoidal wave, 25 cycles/min, to recapitulate the mechanical stress experienced by the alveolar endothelium at high tidal volume mechanical ventilation (32–34). Control BioFlex plates with static EC culture were be placed in the same cell culture incubator. Both static HPAEC cultures and cells exposed to CS were seeded onto identical plates to ensure standard culture conditions. When necessary, static controls and CS-exposed HPAEC were treated with thrombin and incubated under continuous exposure to both stimuli. At the end of experiment, cell lysates were collected for biochemical assays, or CS-exposed endothelial monolayers were fixed with 3.7% formaldehyde and used for immunohistochemistry.

Express Micromolecule Permeability Testing Assay—XPerT, recently developed in our group (35), is based on high affinity binding of avidin-conjugated FITC-labeled tracer added to the culture medium during or after EC treatment with barrier-disruptive agonist to the biotinylated ligand in the underlying matrix. Permeability measurements during cyclic stretch were performed using the 6-well BioFlex plates. HPAEC were seeded on BioFlex plates coated with biotinylated gelatin and grown for 48–72 h followed by exposure to 18% cyclic stretch with or without thrombin treatment on the FX-4000T Flexecell Tension Plus system described above. At the end of the experiment, FITC-avidin (final concentration, 25 μg/ml) was added to the culture medium for 3 min. Unbound FITC-avidin was removed by two-step washing with 3 ml of PBS (37 °C). Elastic bottoms of BioFlex plates with HPAEC were excised with a scalpel and transferred to a polystyrene 6-well cell culture plate. Each membrane was covered with 1 ml of PBS, and the fluorescence of membrane-bound FITC-avidin was measured with Victor X5 multilabel plate reader (PerkinElmer Life Sciences).

Immunofluorescence—Endothelial monolayers grown on BioFlex plates were exposed to cyclic stretch and subjected to immunofluorescence staining as described previously (36). Membranes with attached cells were mounted on 4 × 4-cm rectangular coverslips and analyzed using a Nikon video imaging system (Nikon Instech Co., Tokyo, Japan). Images were processed with ImageJ software (National Institute of Health) and Adobe Photoshop 7.0 (Adobe Systems, San Jose, CA) software. Quantitative analysis of paracellular gap formation and VE-cadherin peripheral accumulation was performed by measurements of junctional VE-cadherin immunoreactivity normalized

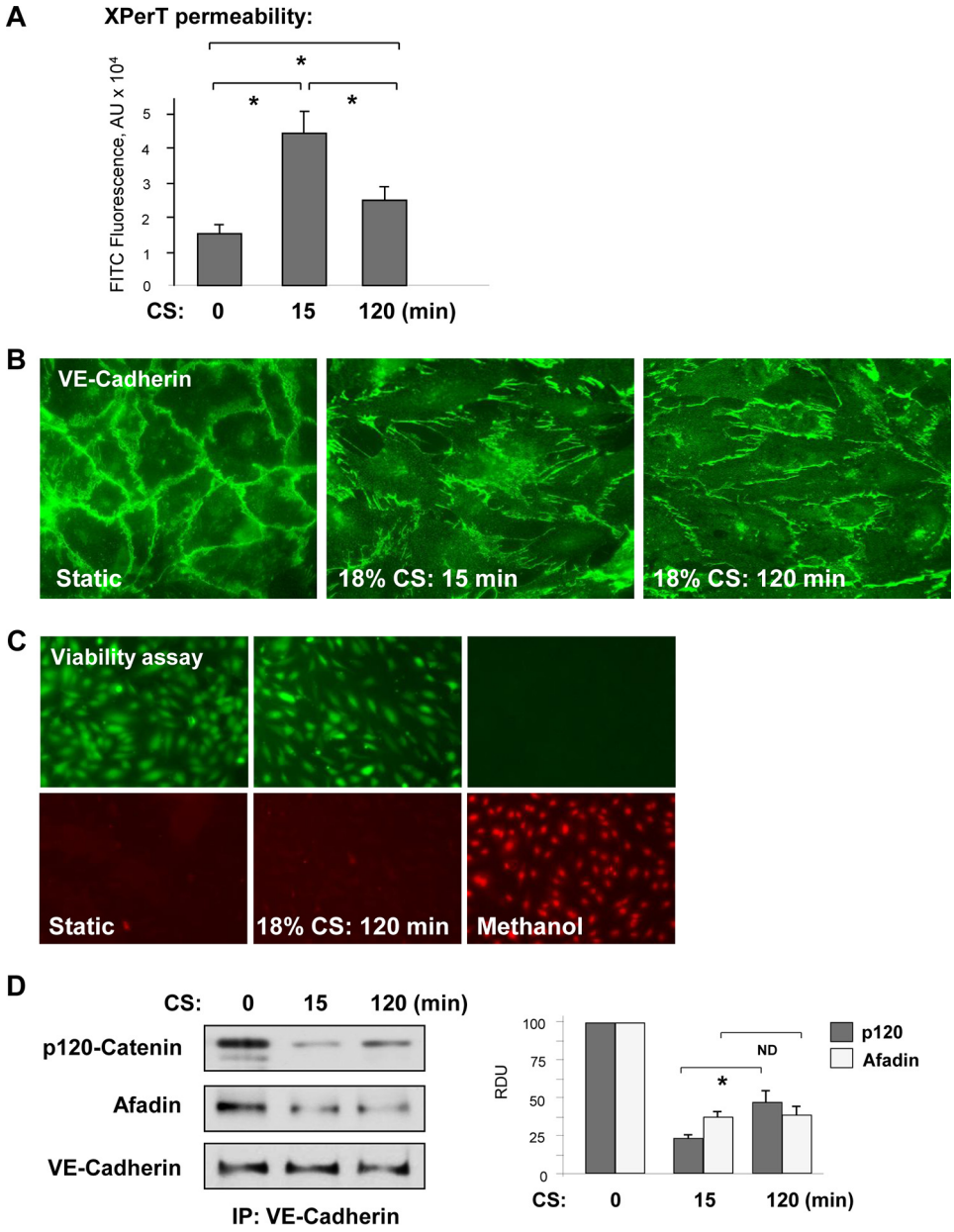

FIGURE 1. **18% CS induced time-dependent changes in EC permeability, monolayer integrity, and adherens junction assembly.** *A*, HPAEC grown in Biofex plates coated with biotinylated gelatin (0.25 mg/ml) were subjected to 18% CS for 15 or 120 min, followed by the addition of FITC-avidin (25 μg/ml, 3 min). Unbound FITC-avidin was removed, and FITC fluorescence was measured. $n = 4$; *, $p < 0.05$. *B*, adherens junction remodeling in control and stretched EC was examined by immunofluorescence staining for VE-cadherin. *C*, cell viability assay. HPAEC were subjected to 18% CS for 120 min or left under static conditions followed by staining with green fluorescent calcein-AM to indicate intracellular esterase activity and red fluorescent ethidium homodimer 1 to indicate loss of plasma membrane integrity. Methanol treatment (50%, 10 min) was used as a control. The results are representative of three independent experiments. *D*, VE-cadherin immunoprecipitation (*IP*) under nondenaturing conditions was performed from control EC or cells subjected to 18% CS. The presence of afadin and p120 catenin in immune complexes was examined by Western blot with corresponding antibody. The bar graph depicts quantitative densitometry analysis of Western blot data. $n = 3$; *, $p < 0.05$.

to square area in control and stimulated cells (32, 37, 38). For each experimental condition, at least 10 microscopic fields in each independent experiment were analyzed.

Differential Protein Fractionation and Immunoblotting—Subcellular protein fractionation was performed as described elsewhere (39). After stimulation with 18% CS and/or thrombin, HPAEC monolayers were washed with ice-cold PBS. The cytosolic fraction was isolated by centrifugation using extraction buffer containing 50 mM Tris-HCl, pH 7.4, 100 mM sodium chloride, 0.01% digitonin, protease, and phosphatase inhibitors mixture. Next, pellets were resuspended in extraction buffer containing 50 mM Tris-HCl, pH 7.4, 2% Triton X-100, 100 mM sodium chloride, protease, and phosphatase inhibitors mixture and incubated on ice for 30 min. The membrane fraction, also containing components of adherens junction complexes and residual components of cortical actin cytoskeleton, was separated from insoluble main cytoskeletal fraction by centrifugation for 5 min at 16,000 $\times$ *g*. For immunoblotting analysis, protein extracts were separated by SDS-PAGE, transferred to PVDF membrane, and probed with specific antibodies. Analy-

sis of the protein phosphorylation profile was performed by membrane probing with phospho-specific antibodies as previously described (40). Equal protein loading was verified by reprobing membranes with antibody to β-actin or specific protein of interest. The relative intensities of immunoreactive protein bands (relative density units) were analyzed and quantified by scanning densitometry using ImageQuant software (Molecular Dynamics, Sunnyvale, CA).

Co-immunoprecipitation—Cells were washed in cold PBS and lysed on ice with cold TBS-Nonidet P-40 lysis buffer (20 mM Tris, pH 7.4, 150 mM NaCl, 1% Nonidet P-40) supplemented with protease and phosphatase inhibitor cocktails (Roche Applied Science). Clarified lysates were then incubated with antibodies to a protein of interest overnight at 4 °C and washed three or four times with TBS-Nonidet P-40 lysis buffer, and the complexes were analyzed by Western blotting using appropriate antibodies.

Surface Protein Biotinylation Assay—The cells exposed to 18% CS or static conditions were washed with PBS (37 °C) and incubated with Sulfo-NHS-SS-Biotin (Pierce) (5 mM, 10 min, room temperature). Subsequently, the cells were washed twice with 100 mM glycine/PBS, lysed in 1% Triton-100/PBS (30 min, on ice) and centrifuged (10,000 × *g*, 10 min, 4 °C). Equal amounts of lysates were incubated with 60 μl of streptavidin-agarose (Pierce) (1 h, 4 °C). The beads were washed three times with ice-cold PBS and boiled in SDS sample buffer with 5% 2-mercaptoethanol. Samples were centrifuged for 1 min at 1,000 × *g*, and supernatants were subjected to Western blotting with antibody of interest.

Statistical Analysis—The results are expressed as means ± S.D. Experimental samples were compared with controls by unpaired Student's *t* test. For multiple group comparisons, a one-way variance analysis and post hoc multiple comparison tests were used. $p < 0.05$ was considered statistically significant.

Results

Transient Increase in EC Permeability Caused by 18% CS Is Associated with Partial Disassembly of Adherens Junctions—We examined the effects of high magnitude CS on EC permeability. Human pulmonary EC grown to confluence on BioFlex plates coated with biotinylated collagen were exposed to 18% CS for 15 or 120 min, and monolayer permeability was evaluated by increased fluorescence of FITC-labeled avidin tracer bound to the bottoms of BioFlex, as described under "Experimental Procedures." Stimulation with 18% CS transiently increased EC monolayer permeability for macromolecules, which declined after 120 min of CS exposure (Fig. 1*A*). The transient permeability increase at 15 min of CS was associated with rapid EC monolayer remodeling, and partial disassembly of adherens junctions was visualized by cell staining for VE-cadherin. In consistence with permeability data, maximal formation of paracellular gaps was observed at 15 min of CS followed by re-establishment of EC monolayer by 120 min (Fig. 1*B*). The viability assay data show no increases in cell death indices in the cells exposed to 120 min of 18% CS (Fig. 1*C*).

Transient effects of 18% CS on AJ integrity were further investigated in co-immunoprecipitation studies. Pulmonary EC were exposed to 18% CS for 15 or 120 min followed by

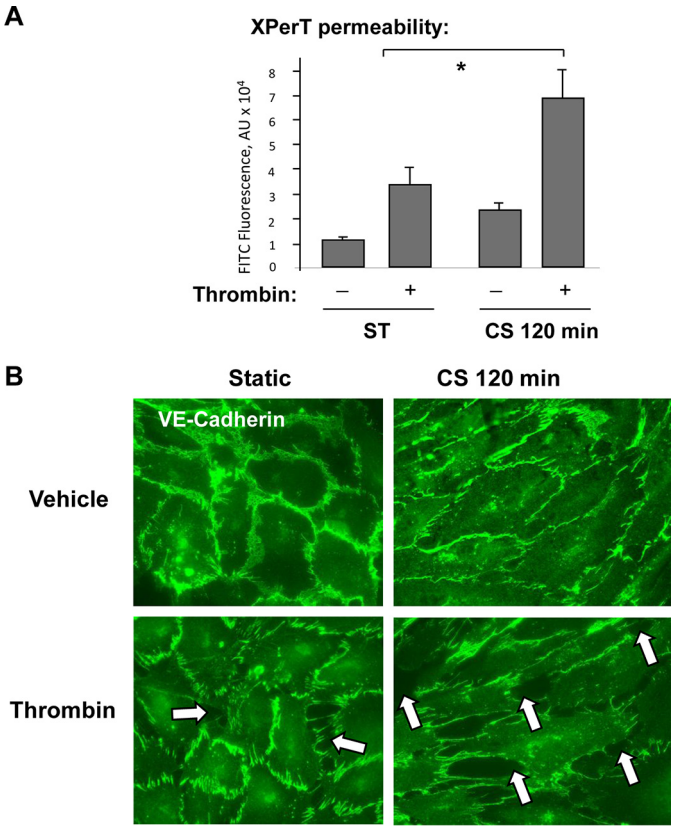

FIGURE 2. **18% CS augmented EC permeability and adherens junction disassembly caused by low dose of thrombin.** HPAEC were subjected to 18% CS for 120 min or left under static (*ST*) conditions, followed by thrombin stimulation (0.1 unit/ml) for the last 15 min of the experiment. *A*, permeability measurements were performed using FITC-avidin fluorescence XPerT assay. $n = 4$; *, $p < 0.05$ *versus* static conditions. *AU*, arbitrary units. *B*, adherens junction remodeling was assessed by immunofluorescence staining for VE-cadherin. The results are representative of three independent experiments (relative density units).

immunoprecipitation of VE-cadherin under nondenaturing conditions. 18% CS induced transient decrease in the amounts of afadin and p120-catenin co-precipitated with VE-cadherin after 15 min of stimulation (Fig. 1*D*). The VE-cadherin·p120-catenin complex was partially restored after 120 min of 18% CS, although the levels of p120-catenin in VE-cadherin immunoprecipitates were lower as compared with static conditions. Afadin association with VE-cadherin remained decreased after 120 min of CS exposure.

Sustained Exposure to 18% CS Augmented EC Permeability Response to Low Dose Thrombin—Stimulation of pulmonary EC exposed to pathologically relevant levels of cyclic stretch with thrombin was used to reproduce a two-hit model of ventilator-induced lung injury (41, 42). Cell monolayers were exposed to 120 min of 18% CS to recapitulate the mechanical stresses experienced by lung endothelium at high tidal volume mechanical ventilation. Prolonged exposure to 18% CS slightly increased basal EC permeability levels but markedly augmented permeability increase caused by low dose of thrombin (0.1 unit/ml) (Fig. 2*A*). At this dose, thrombin caused a submaximal permeability increase in static pulmonary EC culture, which was evaluated by measurements of transendothelial electrical resistance (data not shown). In static EC cultures, stimulation with low thrombin dose caused moderate disruption of adherens

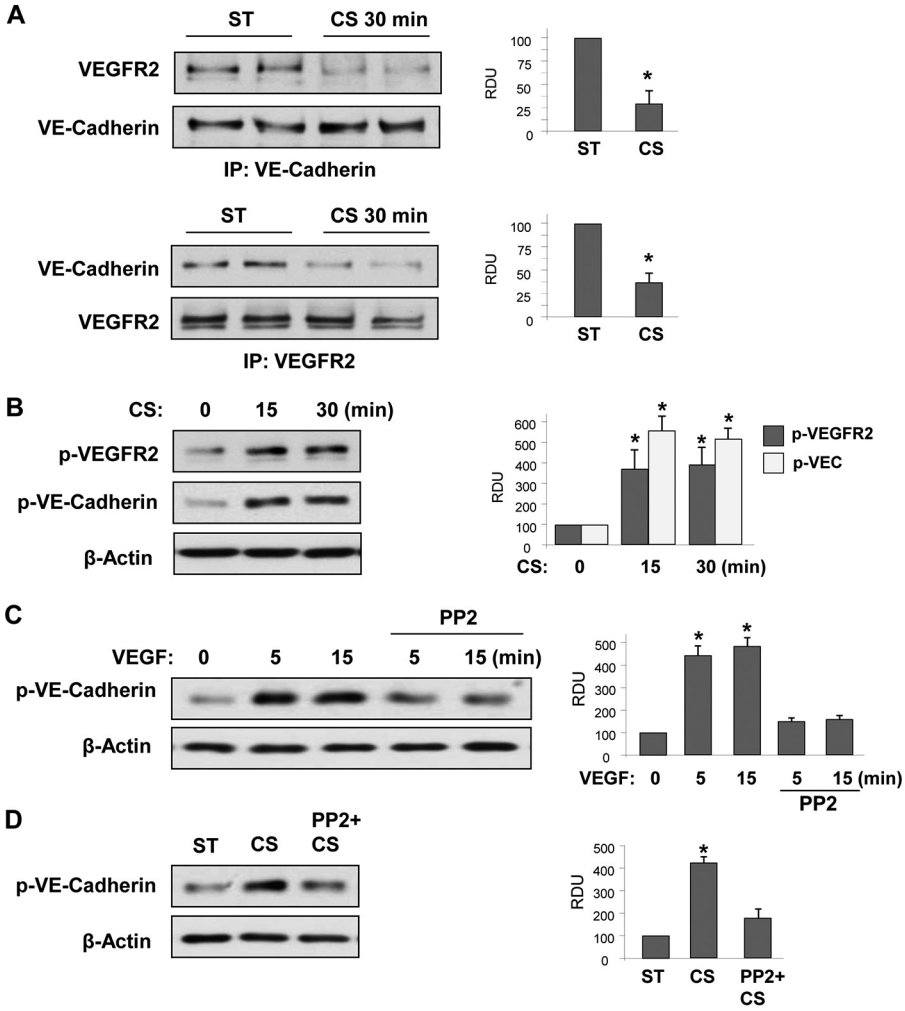

FIGURE 3. **18% CS decreased association between VE-cadherin and VEGFR2 and stimulates their tyrosine phosphorylation.** HPAEC monolayers were stimulated with 18% CS for indicated periods of time or left under static (*ST*) conditions. *A*, co-immunoprecipitation assays using VE-cadherin and VEGFR2 antibodies. The presence of VE-cadherin and VEGFR2 in immunocomplexes was detected by Western blot analysis with corresponding antibody. The bar graphs depict quantitative densitometry analysis of Western blot data. $n = 3$; *, $p < 0.05$ *versus* static conditions. *B*, time-dependent phosphorylation of VEGFR2 and VE-cadherin induced by 18% CS was detected by Western blot analysis with corresponding antibodies. $n = 4$; *, $p < 0.05$ *versus* static conditions. *C*, time-dependent phosphorylation of VE-cadherin in response to VEGF (500 ng/ml) with or without PP2 (2 μm, 30 min) pretreatment was evaluated by Western blot analysis. $n = 3$; *, $p < 0.05$ *versus* VEGF alone. *D*, VE-cadherin phosphorylation was analyzed in 18% CS-exposed EC (15 min) with or without PP2 (2 μm, 30 min) pretreatment. $n = 3$; *, $p < 0.05$ *versus* CS alone. *IP*, immunoprecipitation; *RDU*, relative density units.

junctions detected by VE-cadherin staining. Thrombin-induced disruption of adherens junctions and formation of intercellular gaps were exacerbated in thrombin-treated EC exposed to 18% CS (Fig. 2*B*).

18% CS Caused Dissociation of VE-cadherin·VEGFR2 Complex and Stimulated VEGFR2 and VE-cadherin Tyrosine Phosphorylation and VE-cadherin Internalization—Study of EC monolayers exposed to fluid shear stress demonstrated flow-induced assembly of a VE-cadherin-PECAM1-VEGFR2 complex and defined this complex as a flow-induced mechanosensory module (16). Whether VE-cadherin·VEGFR2 interactions are controlled by cyclic stretch and whether CS-induced VE-cadherin disengagement from AJ induces VEGFR2 activation remain unknown. These questions were addressed in the following studies. 18% CS significantly decreased association of VE-cadherin and VEGFR2 detected in reciprocal co-immunoprecipitation assays probed with VE-cadherin or VEGFR2 antibodies (Fig. 3*A*). 18% CS also caused sustained phosphorylation of VEGFR2 at Tyr^{1175}, which reflects VEGFR2 activation, and increased phosphorylation of VE-cadherin at Tyr^{658} (Fig. 3*B*), which is known to cause VE-cadherin dissociation from p120 catenin, VE-cadherin internalization, and disassembly of adherens junctions (43–45). These results suggest sustained weakening of adherens junction complexes caused by pathologic CS. Because Src family kinases may play a role in VE-cadherin phosphorylation, we next examined whether Src is involved in VEGFR2-mediated phosphorylation of VE-cadherin. VE-cadherin phosphorylation at Tyr^{658} was observed in the cells treated with VEGF. This effect was abolished by Src inhibitor PP2 (Fig. 3*C*). Similarly, pretreatment with Src inhibitor suppressed VE-cadherin phosphorylation in response to CS (Fig. 3*D*).

18% CS-induced VE-cadherin dissociation and VEGFR2 activation were linked to stretch-induced disassembly of VE-cadherin-positive cell junctions (Fig. 1*B*). Interestingly, disengagement of VE-cadherins in static EC culture by cell treatment

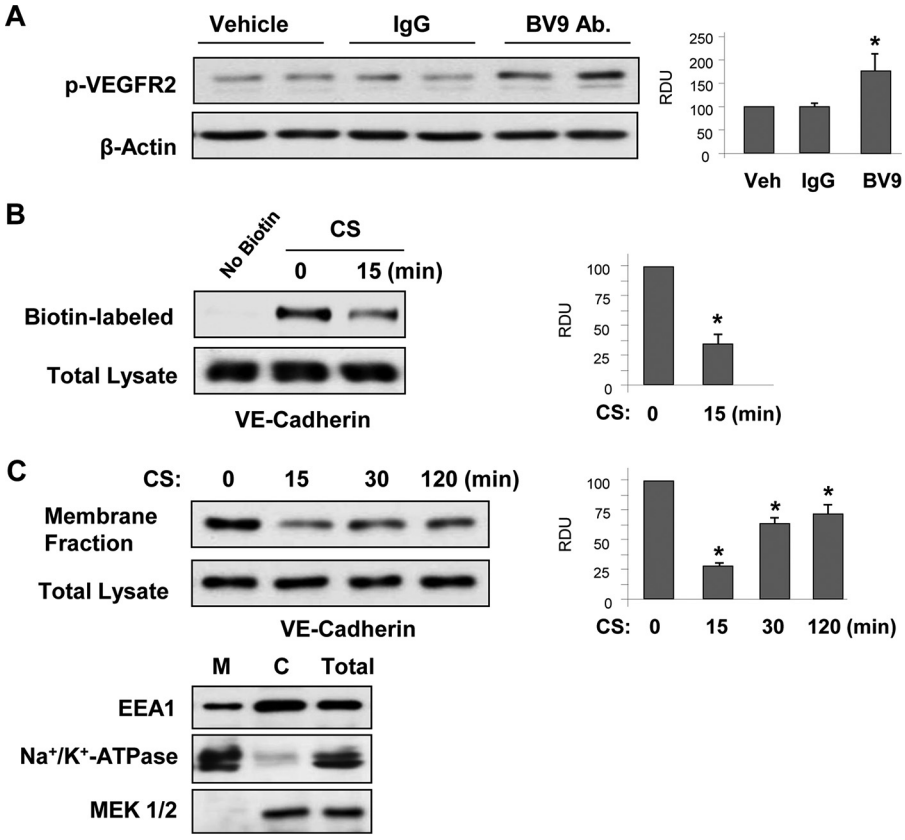

FIGURE 4. **18% CS decreased VE-cadherin internalization.** HPAEC monolayers were stimulated with 18% CS for indicated periods of time or left under static conditions. *A*, phosphorylation of VEGFR2 in static EC after treatment with VE-cadherin extracellular domain blocking antibody BV-9 or control IgG was detected by Western blot. $n = 3$; *, $p < 0.05$ *versus* vehicle. *B*, cell surface proteins were labeled with Sulfo-NHS-SS-Biotin. Biotinylated proteins were collected using streptavidin-agarose, and VE-cadherin content was evaluated by Western blot analysis. $n = 3$; *, $p < 0.05$ *versus* static conditions. *C*, time-dependent VE-cadherin internalization induced by 18% CS was detected by Western blot analysis of VE-cadherin content in the membrane faction and total lysates from control and 18% CS-stimulated EC. $n = 3$; *, $p < 0.05$ *versus* static conditions. Distribution of Na^+/K^+-ATPase, EEA1, and MEK1/2 in cytosolic (*lane C*) and membrane (*lane M*) fractions and total cell lysates was analyzed by Western blot analysis with corresponding antibodies. *Veh*, vehicle.

with BV-9 monoclonal antibody, which blocks homotypic interactions of VE-cadherin extracellular domains with other VE-cadherins and leads to disruption of EC monolayer barrier (46), significantly increased phosphorylation of VEGFR2 (Fig. 4*A*).

Surface biotinylation studies (Fig. 4*B*) showed that 18% CS decreased VE-cadherin membrane localization (Fig. 4*B*). The results were consistent with reduced VE-cadherin content in the membrane fractions. The minimal levels of membrane associated VE-cadherin were observed after 15 min of CS exposure and partially recovered after 2 h of CS stimulation (Fig. 4*C*). Taking into consideration the role of endosomes in VE-cadherin internalization leading to EC barrier dysfunction, we performed an additional characterization of membrane fractions using markers of the plasma membrane and endosomes (Fig. 4*C*). The results show that the membrane fraction preparations contained mostly a plasma membrane marker Na^+/K^+-ATPase and low levels of endosomal marker EEA1, which were most abundant in the cytosolic fraction (47). We did not observe a noticeable decrease of VE-cadherin content in the total cell lysates, suggesting insignificant VE-cadherin degradation in EC exposed to 18% CS. Thus, we interpret changes in VE-cadherin content in the membrane fraction as VE-cadherin dissociation from the plasma membrane, which is also consistent with results of surface biotinylation assays and VE-cadherin immunofluorescence staining.

Mechanical stimulation of EC by flow leads to PECAM1 phosphorylation, which in turn activates Erk kinase cascade. In addition, studies of flow-exposed EC suggest that PECAM1 is a part of the flow-sensing mechanotransduction complex (16, 48, 49). In contrast to recognized PECAM1 role in flow-induced mechanosensing and EC remodeling, the role of PECAM1 in cyclic stretch-induced EC barrier regulation is less well understood. Our experiments show that 18% CS induced PECAM1 phosphorylation (Fig. 5*A*) and partial dissociation from the cell membrane (Fig. 5, *B* and *C*). However, immunoprecipitation experiments (Fig. 5*D*) did not reveal increased PECAM1 association with VE-cadherin or VEGF2 upon acute stimulation with 18% CS. These data were confirmed by imaging analysis of PECAM1 and VE-cadherin localization in the lung EC (Fig. 5*E*). In agreement with previous observations, VE-cadherin was found in immediate adherens junction compartment, whereas PECAM1 was enriched in distinctive areas of overlapping adjacent endothelial cells (57).

VEGFR2 Mediates Stretch-induced VE-cadherin Tyrosine Phosphorylation, Internalization, and Weakening of Adherens Junctions—Does VE-cadherin/VEGFR2 dissociation and VEGFR2 activation represent a mechanism of CS-induced EC permea-

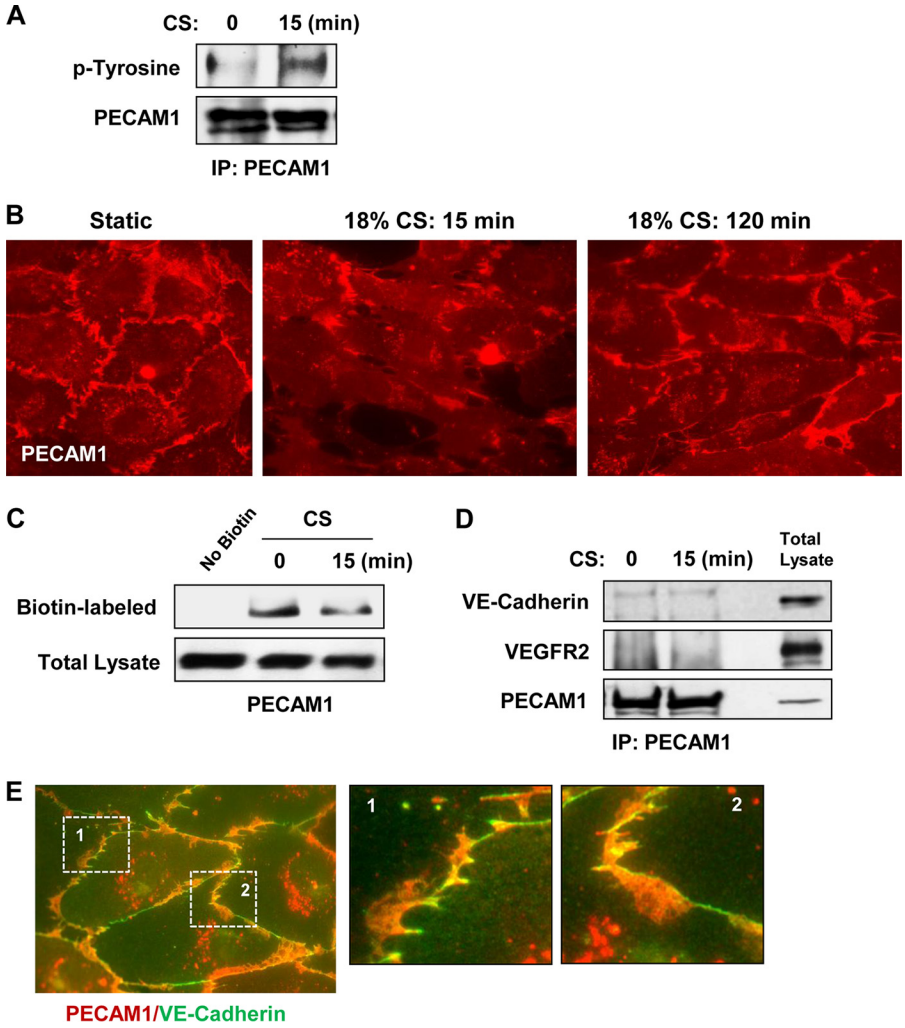

FIGURE 5. **18% CS induced PECAM1 tyrosine phosphorylation and internalization.** HPAEC monolayers were stimulated with 18% CS for indicated periods of time or left under static conditions. *A*, 18% CS-induced PECAM1 tyrosine phosphorylation was analyzed by immunoprecipitation (*IP*) assays with PECAM1 antibody followed by probing for phosphotyrosine. The results are representative of three independent experiments. *B*, PECAM1 distribution in control and stretched EC was examined by immunofluorescence staining. The bar graph represents quantitative analysis of PECAM1 peripheral accumulation. The data are expressed as means ± S.D. of three independent experiments; *, $p < 0.05$ *versus* ns-RNA. *C*, cell surface proteins were labeled with Sulfo-NHS-SS-Biotin. Biotinylated proteins were collected using streptavidin-agarose, and PECAM1 content was evaluated by Western blot analysis with corresponding antibodies. *D*, PECAM1 immunoprecipitation under nondenaturing conditions was performed from control EC or cells subjected to 18% CS for 15 min. The presence of VEGFR2 and VE-cadherin in immune complexes was examined by Western blot. *E*, PECAM1 and VE-cadherin co-localization in lung EC was examined by double immunofluorescence staining for PECAM1 (*red*) and VE-cadherin (*green*). *Insets*, higher magnification images of peripheral cell areas marked by quadrangles.

bility? To address this question, we performed experiments with molecular and pharmacological inhibition of VEGFR2. siRNA-induced knockdown of VEGFR2 in pulmonary EC monolayers prior to their exposure to 18% CS abrogated stretch-induced phosphorylation of VE-cadherin at Tyr^{658} (Fig. 6*A*). Similar inhibition of CS-induced VE-cadherin phosphorylation was observed in EC treated with VEGF receptor inhibitor, SU-1498 (Fig. 6*B*). Suppression of CS-induced VE-cadherin phosphorylation by inhibition of VEGFR2 signaling led to increased VE-cadherin cell membrane localization detected by subcellular fractionation assays (Fig. 6*C*) and improved assembly of VE-cadherin-positive adherens junctions shown by immunofluorescence staining of EC monolayers for VE-cadherin (Fig. 6*D*).

VEGFR2 Mediates Exacerbation of Cyclic Stretch-induced EC Permeability Caused by Thrombin—Involvement of VEGFR2 in exacerbation of agonist-induced EC permeability by 18% CS was tested in experiments with VEGFR2 knockdown. CS-stimulated cells treated with control and VEGFR2-specific siRNA we challenged with submaximal doses of thrombin (0.1 unit/ml). EC permeability was assessed using fluorescence-based XPerT permeability assay described above. VEGFR2 knockdown decreased the permeability response to combined stimulation of EC with 18% CS and thrombin (Fig. 7*A*). VEGFR2 knockdown also abolished 18% CS/thrombin-induced disappearance of VE-cadherin from the cell membrane fraction (Fig. 7*B*) and suppressed formation of paracellular gaps in EC monolayers exposed to 18% CS and thrombin, as shown by visualization of VE-cadherin positive adherens junctions (Fig. 7*C*).

Role of Afadin in Preservation of the Integrity of the VEGFR2·VE-cadherin Complex and Adherens Junction in EC Exposed to 18% CS—Afadin is an important initiator of cell junction assembly. Afadin association with VE-cadherin and p120-catenin plays a key role in the maintenance of cell monolayer

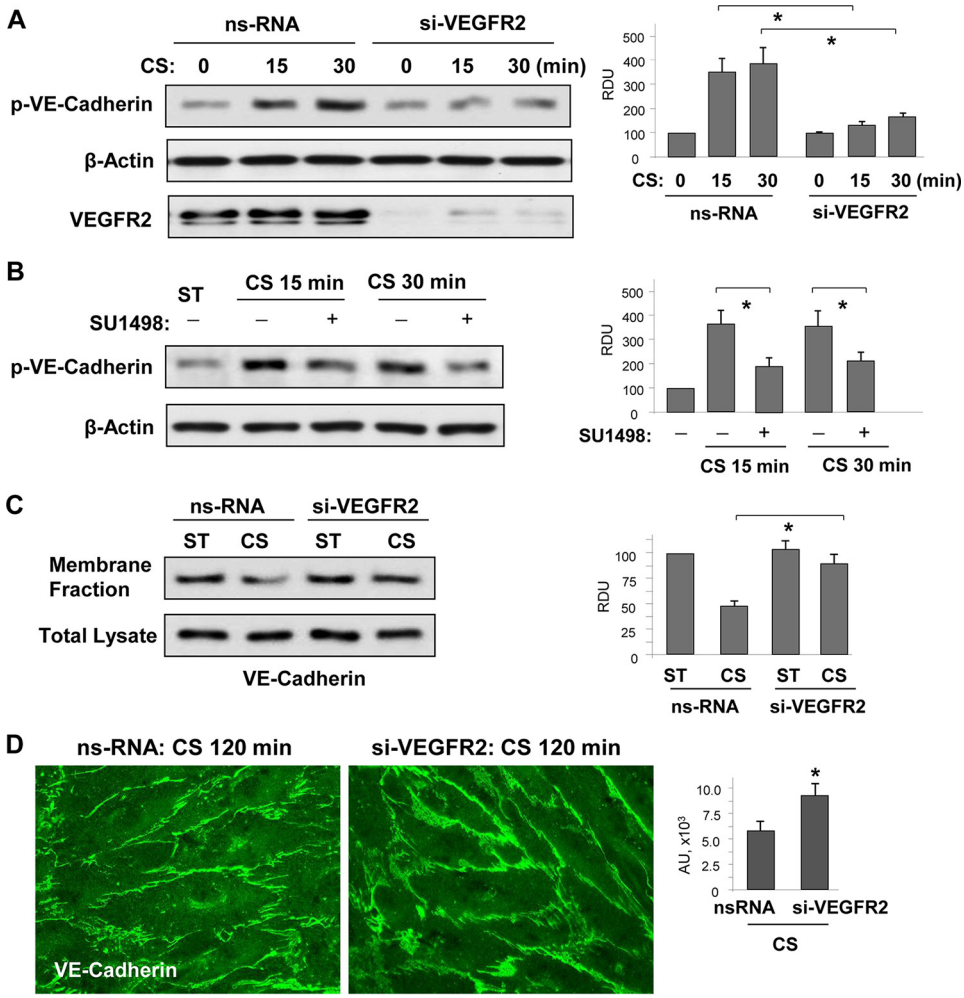

FIGURE 6. **18% CS-induced VEGFR2 activation mediated VE-cadherin phosphorylation, internalization, and disassembly of adherens junctions.** Human pulmonary EC were transfected with VEGFR2-specific or nonspecific siRNA, followed by 18% CS stimulation for indicated periods of time. Control cells were left under static conditions. *A*, effect of VEGFR2 knockdown on CS-induced VE-cadherin tyrosine phosphorylation. siRNA-induced protein depletion was confirmed by Western blot. *β*-Actin was used as a normalization control. $n = 3$; *, $p < 0.05$ *versus* ns-RNA. *B*, effect of inhibition of VEGFR2 tyrosine kinase activity on CS-induced VE-cadherin tyrosine phosphorylation. The cells were treated with vehicle or 5 μM SU-1498 for 30 min prior to exposure to cyclic stretch. VE-cadherin phosphorylation was analyzed by Western blot with corresponding antibody. *β*-Actin was used as a normalization control. $n = 3$; *, $p < 0.05$ *versus* 18% CS alone. *C*, effect of VEGFR2 knockdown on 18% CS-induced VE-cadherin internalization was detected by Western blot analysis of protein content in the membrane faction and total lysates from static and stretched EC. $n = 3$; *, $p < 0.05$ *versus* ns-RNA. *D*, effect of VEGFR2 knockdown on 18% CS-induced adherence junction remodeling was evaluated by immunofluorescence staining of EC monolayers with VE-cadherin antibody. The bar graph represents quantitative analysis of VE-cadherin peripheral accumulation. The data are expressed as means ± S.D. of three independent experiments; *, $p < 0.05$ *versus* ns-RNA.

integrity (11, 50). The data described above (Fig. 1) show that EC exposure to 18% CS caused transient disassembly of the VE-cadherin·afadin·p120-catenin complex. The dissociation of afadin from VE-cadherin induced by 18% CS was inhibited in EC with VEGFR2 knockdown (Fig. 8*A*), which is consistent with the preservation of adherens junction integrity and EC barrier in CS-stimulated EC with VEGFR2 knockdown (Figs. 5 and 6).

Afadin is also known to enhance the EC barrier by promoting physical interactions between adherens junctions and tight junctions (13, 51). Based on these properties of afadin, we questioned whether altered afadin expression may affect EC monolayer barrier properties under mechanical forces. Experiments with afadin knockdown showed increased VEGFR2 and VE-cadherin phosphorylation in EC exposed to 18% CS (Fig. 8*B*), accompanied by impaired recovery of adherens junction complexes after 120 min of stretching (Fig. 8*C*). Next, we examined whether enhancement of cell junction complexes by forced afadin expression may preserve VE-cadherin·VEGFR2 association and thus maintain the integrity of EC monolayers exposed to pathologic CS. Expression of recombinant afadin suppressed CS-induced disassembly of the VEGFR2·VE-cadherin complex as detected by co-immunoprecipitation assay with VEGFR2 antibody (Fig. 9*A*). The preservation of this complex was accompanied by inhibition of 18% CS-induced tyrosine phosphorylation of VEGFR2 and VE-cadherin (Fig. 9*B*). Ectopic expression of afadin also increased the pool of membrane-associated VE-cadherin in static EC cultures and stabilized VE-cadherin in the membrane fraction of EC monolayers exposed to 18% CS (Fig. 9*C*). These results suggest a role for afadin in the stabilization of surface VE-cadherin and preservation of EC barrier integrity.

Discussion

Increased lung vascular leak caused by lung microvascular overdistension during mechanical ventilation at high tidal vol-

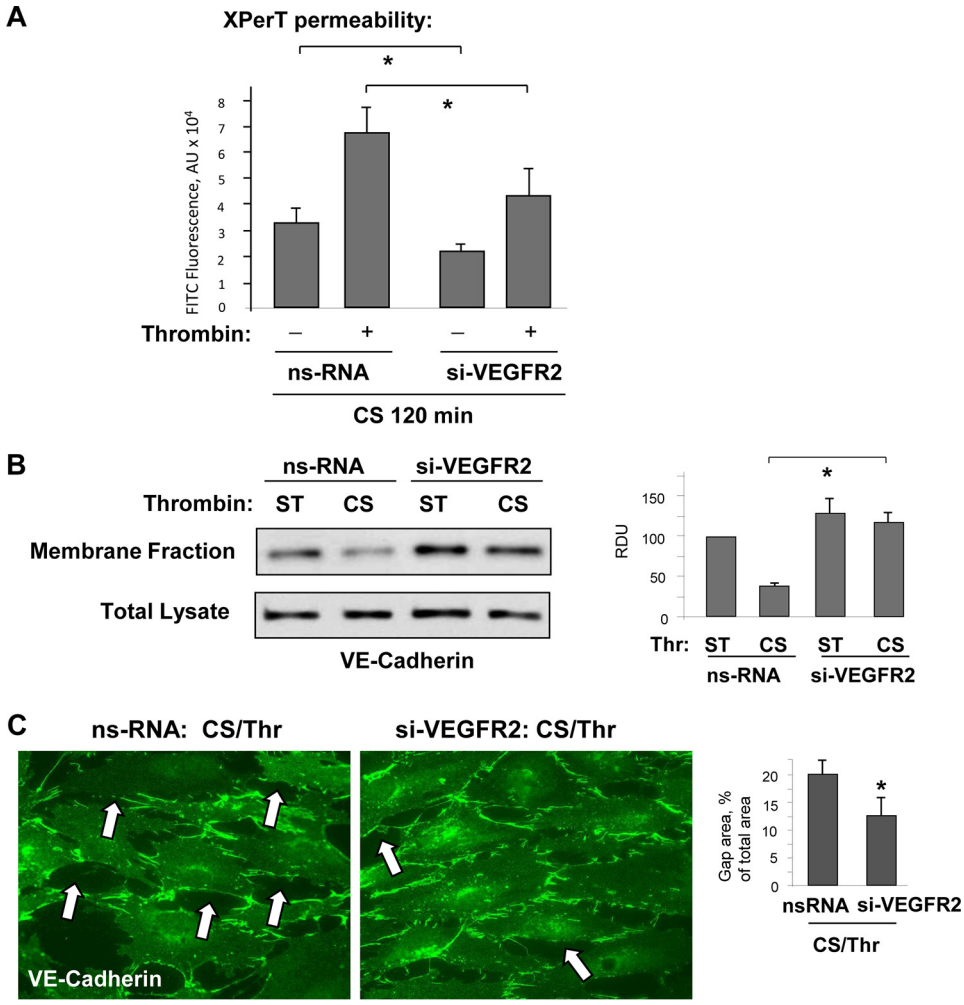

FIGURE 7. **VEGFR2 knockdown attenuated synergistic effect of 18% CS on EC permeability and VE-cadherin internalization induced by low dose thrombin.** HPAEC were transfected with VEGFR2-specific or nonspecific siRNA, followed by application of 18% CS for 120 min. Vehicle or thrombin (0.1 unit/ml) were added for the last 15 min of the experiment. *A*, permeability measurements were performed using FITC-avidin fluorescence XPerT assay. $n = 4$; *, $p < 0.05$ *versus* ns-RNA. *B*, VE-cadherin internalization was assessed by Western blot analysis of protein content in the membrane faction and total lysates from static (*ST*) and stretched EC stimulated with thrombin. $n = 3$; *, $p < 0.05$ *versus* ns-RNA. *C*, effect of VEGFR2 knockdown on EC monolayer gap formation caused by 18% CS, and thrombin was evaluated by immunofluorescence staining of EC monolayers with VE-cadherin antibody. Paracellular gaps are marked by *arrows*. The bar graph represents quantitative analysis of paracellular gap formation. The data are expressed as means ± S.D. of three independent experiments. *, $p < 0.05$ *versus* ns-RNA.

ume is a result of stretch-induced EC barrier dysfunction. EC exposed to pathologic mechanical forces become more susceptible to barrier-disruptive agonists. The mechanism of such sensitization remains unclear. This study demonstrates for the first time the sustained CS-induced weakening of adherens junctions in pulmonary EC and describes a molecular mechanism of prolonged vascular leak caused by excessive mechanical strain.

Rapid EC barrier dysfunction caused by short term CS is associated with EC reorientation response and mediated mostly by Rho mechanisms (36). Our new data show that even after 2 h of 18% CS, when acute barrier disruption and cytoskeletal remodeling driven by Rho mechanisms subsides, continuing exposure to pathologically relevant high CS increases endothelial permeability and weakens VE-cadherin adherens junctions. This conclusion is supported by decreased intensity of VE-cadherin immunofluorescence signal at the cell junctions, decreased content of AJ proteins p120-catenin and afadin in VE-cadherin immunoprecipitates, and the decreased pool of membrane-localized VE-cadherin in CS-stimulated EC monolayers.

VEGFR2 mediates VEGF-induced EC permeability by several mechanisms including the RhoA pathway (52, 53). Interestingly, VEGFR2 activity is negatively regulated by VEGFR2 association with VE-cadherin at adherens junctions. The presence of VE-cadherin attenuates VEGF-induced VEGFR2 tyrosine phosphorylation and VEGFR2-mediated signaling (17, 54). Our data show that 18% CS caused sustained tyrosine phosphorylation of VE-cadherin and VEGFR2 and decreased VE-cadherin·VEGFR2 association. CS exposure also increased EC sensitivity to the barrier-disruptive effect of thrombin. Increased sensitivity of CS-preconditioned EC to agonist stimulation and exacerbation of barrier-disruptive response may reflect a change in signaling "setting points" brought by cell exposure to the physiologic or pathologic mechanical environment, which may shift the balance of basal intracellular signaling, such as stretch-activated channel activity, basal activities of small GTPases, and gene expression. These effects of cyclic

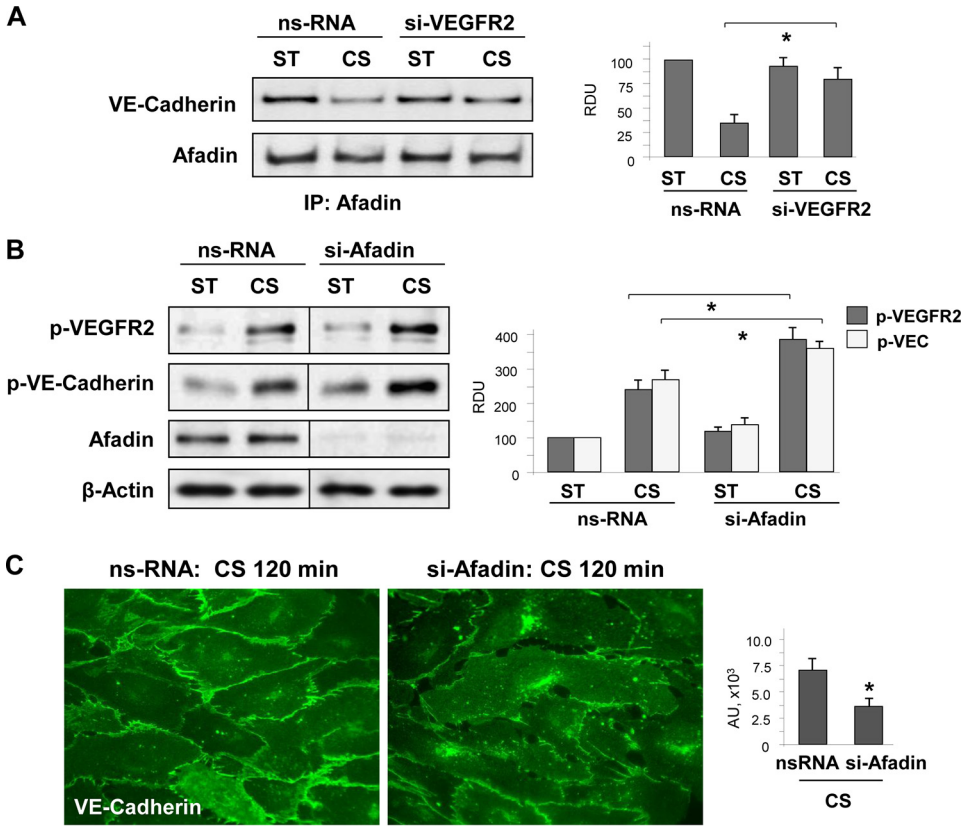

FIGURE 8. **Effect of afadin depletion on VE-cadherin and VEGFR2 association phosphorylation EC monolayer recovery under 18% CS.** *A*, HPAEC transfected with VEGFR2-specific or nonspecific siRNA were left static (*ST*) or exposed to 18% CS (120 min). Afadin association with VE-cadherin in static and 18% CS-stimulated EC was evaluated by co-immunoprecipitation assay using afadin antibody. $n = 3$; *, $p < 0.05$ *versus* ns-RNA. *B* and *C*, EC were transfected with afadin-specific or nonspecific siRNA, followed by 18% CS stimulation. Control cells were left under static conditions. *B*, effect of afadin knockdown on CS-induced (15 min) VEGFR2 and VE-cadherin tyrosine phosphorylation. siRNA-induced protein depletion was confirmed by Western blot. β-Actin was used as a normalization control. $n = 3$; *, $p < 0.05$ *versus* ns-RNA. *C*, effect of afadin knockdown on 18% CS-induced (120 min) adherence junction remodeling was evaluated by immunofluorescence staining of EC monolayers with VE-cadherin antibody. The bar graph represents quantitative analysis of VE-cadherin peripheral accumulation. The data are expressed as means ± S.D. of three independent experiments. *, $p < 0.05$ *versus* ns-RNA. *IP*, immunoprecipitation.

stretch and flow preconditioning have been described in the literature (55–57). Altogether, changing set points of sensitivity to circulating agonists by organ or vessel exposure to physiologic or pathologic mechanical forces may be an important factor defining specific responses to external stimuli. In the present model, such sensitization of agonist-induced barrier disruption may be due to CS-induced activation of VEGFR2 signaling, which is known to stimulate vascular permeability or increased VE-cadherin internalization. VE-cadherin tyrosine phosphorylation also decreased VE-cadherin association with other AJ binding partners (p120-catenin and afadin) and the membrane-associated pool of VE-cadherin.

CS-induced phosphorylation of VE-cadherin at Tyr^{658} was mediated by VEGFR2, as shown by experiments with siRNA-induced VEGFR2 knockdown or pharmacological inhibition VEGFR2 tyrosine kinase activity by SU-1498. Our data also demonstrate that VEGFR2-mediated VE-cadherin phosphorylation is Src-dependent: (*a*) VE-cadherin was phosphorylated upon cells stimulation with VEGF; this effect was abolished by Src inhibitor; and (*b*) pretreatment with Src inhibitor suppressed CS-induced VE-cadherin phosphorylation. These results demonstrate a signaling mechanism of VEGFR2-mediated Src-dependent VE-cadherin phosphorylation (58, 59). The importance of AJ-associated VE-cadherin for the control of VEGFR2 activity is further illustrated by experiments with EC incubation with VE-cadherin blocking antibody BV-9, which significantly increased VEGFR2 tyrosine phosphorylation. BV-9 binds to cell surface-exposed VE-cadherin, leading to AJ disassembly, VE-cadherin internalization, and increased EC permeability (46).

It is currently known that mechanosensory complex of PECAM1, VEGFR2, Src, and VE-cadherin confers endothelial responsiveness to shear stress and activates proinflammatory signaling pathways in response to disturbed flow (16). Although previous works described distinct VE-cadherin and PECAM1 localization under basal conditions (60, 61), recent studies of vascular EC response to fluid shear stress reported assembly of mechanosensory complex consisting of PECAM1, VE-cadherin, and VEGFR2 (16, 62). It was also shown that PECAM1 recruits protein-tyrosine phosphatase SHP-2 in response to flow shear stress and thus activates Erk MAP kinase signaling (63). PECAM1 is phosphorylated by both shear stress and CS (64). The elegant study by the Fujiwara group (64) demonstrated that CS may cause PECAM1 phosphorylation even in Triton-permeabilized cell models in the presence of ATP. Specific analysis of PECAM1 dynamics during 18% CS-induced EC barrier dysfunction showed CS-induced PECAM1 phosphorylation, disappearance from the cell periphery, and PECAM1

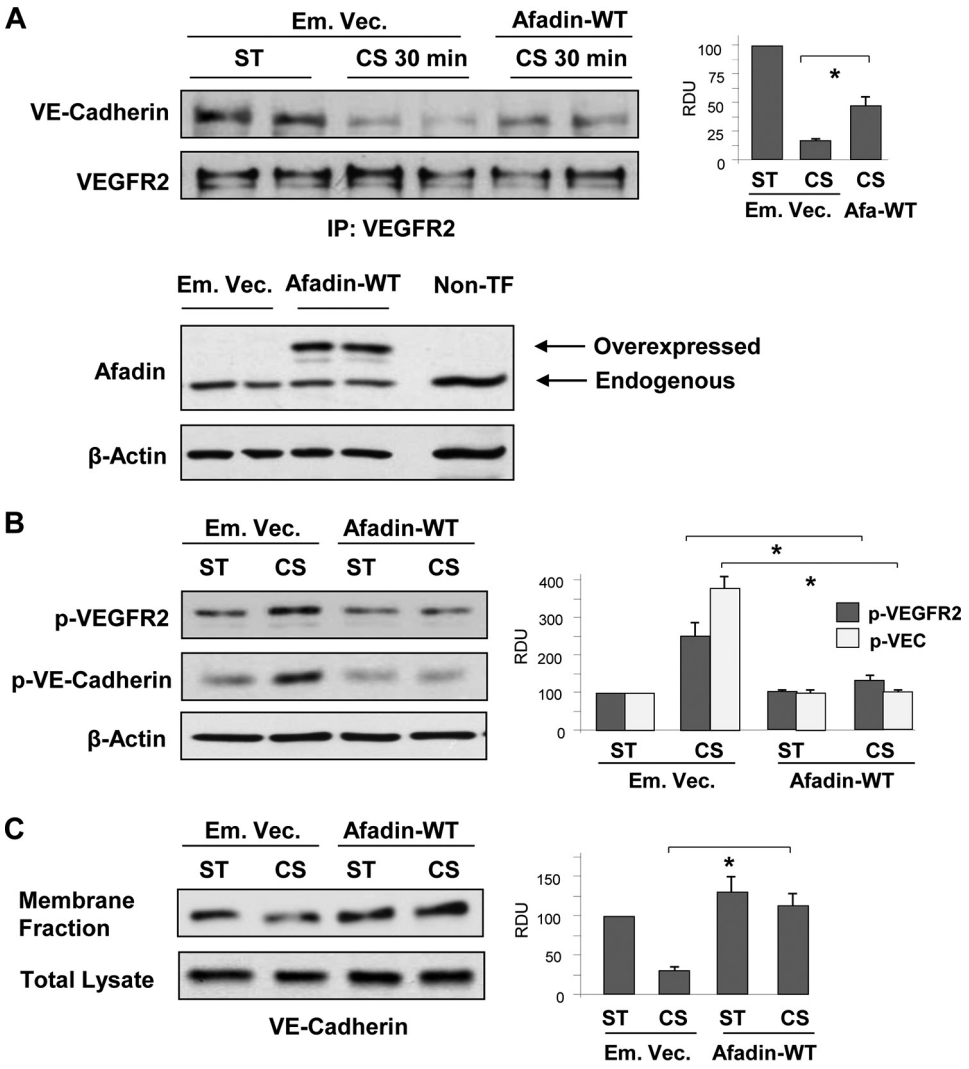

FIGURE 9. **Effect of afadin expression on VE-cadherin·VEGFR2 association and tyrosine phosphorylation under 18% CS.** *A*, HPAEC were transiently transfected with EGFP-tagged wild type afadin (Afadin-WT) or empty vector (*Em. Vec.*), followed by stimulation with 18% CS for 30 min or static (*ST*) conditions. VE-cadherin·VEGFR2 association in static and 18% CS-stimulated EC was evaluated by co-immunoprecipitation assay using VEGFR2 antibody. $n = 3$; *, $p < 0.05$ *versus* empty vector. Ectopic expression of wild type afadin in pulmonary EC was verified by Western blot analysis of total lysates. *B*, HPAEC were transfected with empty vector or wild type afadin and then stimulated with 18% CS for 120 min or left under static conditions. 18% CS-induced tyrosine phosphorylation of VEGFR2 and VE-cadherin in control and adafin expressing EC was evaluated by Western blot with corresponding antibodies. $n = 3$; *, $p < 0.05$ *versus* empty vector. *C*, VE-cadherin internalization was detected by Western blot analysis of protein content in the membrane faction and total lysates from static and stretched EC (18% CS, 120 min) transfected with empty vector or wild type afadin. $n = 3$; *, $p < 0.05$ *versus* empty vector. *IP*, immunoprecipitation.

internalization (Fig. 5). However, immunoprecipitation and imaging studies did not reveal increased PECAM1 association with VE-cadherin or VEGF2 upon stimulation with 18% CS. In our model, acute high magnitude CS caused rapid disruption of cell junctions not observed after shear stress application. These results reflect different effects of shear stress and cyclic stretch on assembly of this mechanotransduction complex. Moreover, acute exposure to CS and shear stress induces different cytoskeletal responses: Rac-dependent formation of lamellipodia-like structures and barrier enhancement response by flow-stimulated EC (65) *versus* RhoA-dependent remodeling of stress fibers and disassembly of cell junctions in EC exposed to acute stretching at pathologically relevant magnitude (20, 26, 66). Therefore, both types of mechanical loads on vascular endothelium share common and distinct mechanotransduction mechanisms affecting EC physiology and functional responses to agonists. The current study provides new information about functioning of this signaling module in EC exposed to 18% CS and demonstrates a novel role of VEGFR2·VE-cadherin complex in EC adaptation and agonist-induced permeability responses under high magnitude CS. The role of PECAM1-triggered signaling in high magnitude CS-mediated EC barrier disruption is an interesting question that requires further investigation.

Another novel finding of this study is the preservation of monolayer integrity in CS-stimulated EC monolayers by forced expression of afadin, which rescued EC barrier disruption caused by high magnitude CS. Afadin is a scaffold protein mediating assembly of cell-cell junctions (12). Our recent study shows that afadin promotes association between p120-catenin and VE-cadherin and contributes to agonist-induced EC barrier enhancement (13). The present study shows the protective effect of forced afadin expression: an attenuation of CS-induced VEGFR2 and VE-cadherin phosphorylation and CS-induced

dissociation of the VE-cadherin·VEGFR2 complex. In contrast, afadin knockdown augmented VEGFR2 and VE-cadherin phosphorylation in response to acute 18% CS and decreased recovery of adherens junction complexes after 2 h of stretching. These effects are most likely dictated by afadin function as a scaffold protein that stabilizes VE-cadherin adherens junctions and maintains the barrier in EC monolayers exposed to prolonged CS. Taken together, the data strongly suggest that the VEGFR2·VE-cadherin uncoupling at cell junctions caused by excessive cyclic stretch leads to VEGFR2 activation, VE-cadherin phosphorylation, and propagation of barrier-disruptive signaling cascade. It is also important to note that activation of the VEGF-VEGFR2 pathway stimulates Rho-dependent signaling, which may also affect EC permeability. Therefore, CS-induced and VEGFR2-dependent AJ weakening and additional stimulation of Rho pathway may cause a synergistic effect on EC permeability and further augment the effects of barrier-disruptive agonists.

Based on our results, we propose a model of impaired EC permeability caused by sustained pathologically relevant excessive cyclic stretch. The cyclic nature of vascular mechanical strain in pathologic conditions, for example during suboptimal mechanical ventilation, maintains certain levels of AJ disruption, which cause continuing physical disassembly of VE-cadherin-positive AJs. Uncoupling of the AJ-associated VE-cadherin·VEGFR2 complex leads to autoactivation of VEGFR2 by tyrosine phosphorylation at Tyr^{1175} (67). In turn, activated VEGFR2 stimulates Src-dependent tyrosine phosphorylation of VE-cadherin at the p120-catenin binding site Tyr^{658}, which causes p120-catenin dissociation from VE-cadherin and promotes further disassembly of AJ. This process is also accompanied by CS-induced phosphorylation and internalization of PECAM1. Forced expression of adaptor protein afadin physically enhances cell junctions, increases VE-cadherin·VEGFR2 interactions, and resolves CS-stimulated barrier-disruptive VEGFR2 signaling. As an alternative, the vicious circle of high magnitude CS-induced AJ weakening and ventilator-induced lung vascular leak *in vivo* may be blocked by pharmacological activation of Rap1 and Rac1 pathways (31, 42, 68, 69), which stimulate cell junction assembly (70–72), or by increased expression of AJ- and TJ-associated structural proteins.

Author Contributions—Y. T., G. G., and J. J. O. performed and analyzed the experiments and contributed to the preparation of the figures. A. A. B. and K. G. B. designed the study, analyzed data, and wrote the manuscript. All authors reviewed the results and approved the final version of the manuscript.

Acknowledgment—We thank Nicolene Sarich for superb laboratory assistance.

References

1. Uhlig, S. (2002) Ventilation-induced lung injury and mechanotransduction: stretching it too far? *Am. J. Physiol. Lung Cell Mol. Physiol.* **282,** L892–L896
2. Slutsky, A. S., and Tremblay, L. N. (1998) Multiple system organ failure: is mechanical ventilation a contributing factor? *Am. J. Respir. Crit. Care Med.* **157,** 1721–1725
3. Bazzoni, G., and Dejana, E. (2004) Endothelial cell-to-cell junctions: molecular organization and role in vascular homeostasis. *Physiol. Rev.* **84,** 869–901
4. Vandenbroucke, E., Mehta, D., Minshall, R., and Malik, A. B. (2008) Regulation of endothelial junctional permeability. *Ann. N.Y. Acad. Sci.* **1123,** 134–145
5. Weber, C., Fraemohs, L., and Dejana, E. (2007) The role of junctional adhesion molecules in vascular inflammation. *Nat. Rev. Immunol.* **7,** 467–477
6. Prasain, N., and Stevens, T. (2009) The actin cytoskeleton in endothelial cell phenotypes. *Microvasc. Res.* **77,** 53–63
7. Gavard, J. (2014) Endothelial permeability and VE-cadherin: a wacky comradeship. *Cell Adh. Migr.* **8,** 158–164
8. Birukova, A. A., Tian, Y., Dubrovskyi, O., Zebda, N., Sarich, N., Tian, X., Wang, Y., and Birukov, K. G. (2012) VE-cadherin trans-interactions modulate Rac activation and enhancement of lung endothelial barrier by iloprost. *J. Cell Physiol.* **227,** 3405–3416
9. Nawroth, R., Poell, G., Ranft, A., Kloep, S., Samulowitz, U., Fachinger, G., Golding, M., Shima, D. T., Deutsch, U., and Vestweber, D. (2002) VE-PTP and VE-cadherin ectodomains interact to facilitate regulation of phosphorylation and cell contacts. *EMBO J.* **21,** 4885–4895
10. Coon, B. G., Baeyens, N., Han, J., Budatha, M., Ross, T. D., Fang, J. S., Yun, S., Thomas, J. L., and Schwartz, M. A. (2015) Intramembrane binding of VE-cadherin to VEGFR2 and VEGFR3 assembles the endothelial mechanosensory complex. *J. Cell Biol.* **208,** 975–986
11. Takai, Y., and Nakanishi, H. (2003) Nectin and afadin: novel organizers of intercellular junctions. *J. Cell Sci.* **116,** 17–27
12. Tawa, H., Rikitake, Y., Takahashi, M., Amano, H., Miyata, M., Satomi-Kobayashi, S., Kinugasa, M., Nagamatsu, Y., Majima, T., Ogita, H., Miyoshi, J., Hirata, K., and Takai, Y. (2010) Role of afadin in vascular endothelial growth factor- and sphingosine 1-phosphate-induced angiogenesis. *Circ. Res.* **106,** 1731–1742
13. Birukova, A. A., Fu, P., Wu, T., Dubrovskyi, O., Sarich, N., Poroyko, V., and Birukov, K. G. (2012) Afadin controls p120-catenin-ZO-1 interactions leading to endothelial barrier enhancement by oxidized phospholipids. *J. Cell Physiol.* **227,** 1883–1890
14. Tsukita, S., Katsuno, T., Yamazaki, Y., Umeda, K., Tamura, A., and Tsukita, S. (2009) Roles of ZO-1 and ZO-2 in establishment of the belt-like adherens and tight junctions with paracellular permselective barrier function. *Ann. N.Y. Acad. Sci.* **1165,** 44–52
15. Harris, E. S., and Nelson, W. J. (2010) VE-cadherin: at the front, center, and sides of endothelial cell organization and function. *Curr. Opin. Cell Biol.* **22,** 651–658
16. Tzima, E., Irani-Tehrani, M., Kiosses, W. B., Dejana, E., Schultz, D. A., Engelhardt, B., Cao, G., DeLisser, H., and Schwartz, M. A. (2005) A mechanosensory complex that mediates the endothelial cell response to fluid shear stress. *Nature* **437,** 426–431
17. Lampugnani, M. G., Orsenigo, F., Gagliani, M. C., Tacchetti, C., and Dejana, E. (2006) Vascular endothelial cadherin controls VEGFR-2 internalization and signaling from intracellular compartments. *J. Cell Biol.* **174,** 593–604
18. Birukova, A. A., Lee, S., Starosta, V., Wu, T., Ho, T., Kim, J., Berliner, J. A., and Birukov, K. G. (2012) A role for VEGFR2 activation in endothelial responses caused by barrier disruptive OxPAPC concentrations. *PLoS One* **7,** e30957
19. Cavanaugh, K. J., Jr., and Margulies, S. S. (2002) Measurement of stretch-induced loss of alveolar epithelial barrier integrity with a novel in vitro method. *Am. J. Physiol. Cell Physiol.* **283,** C1801–C1808
20. Birukova, A. A., Chatchavalvanich, S., Rios, A., Kawkitinarong, K., Garcia, J. G., and Birukov, K. G. (2006) Differential regulation of pulmonary endothelial monolayer integrity by varying degrees of cyclic stretch. *Am. J. Pathol.* **168,** 1749–1761
21. Abdulnour, R. E., Peng, X., Finigan, J. H., Han, E. J., Hasan, E. J., Birukov, K. G., Reddy, S. P., Watkins, J. E., 3rd, Kayyali, U. S., Garcia, J. G., Tuder, R. M., and Hassoun, P. M. (2006) Mechanical stress activates xanthine oxidoreductase through MAP kinase-dependent pathways. *Am. J. Physiol. Lung Cell Mol. Physiol.* **291,** L345–L353

22. DiPaolo, B. C., and Margulies, S. S. (2012) Rho kinase signaling pathways during stretch in primary alveolar epithelia. *Am. J. Physiol. Lung Cell Mol. Physiol.* **302,** L992–L1002
23. Cohen, T. S., Cavanaugh, K. J., and Margulies, S. S. (2008) Frequency and peak stretch magnitude affect alveolar epithelial permeability. *Eur. Respir. J.* **32,** 854–861
24. Iwaki, M., Ito, S., Morioka, M., Iwata, S., Numaguchi, Y., Ishii, M., Kondo, M., Kume, H., Naruse, K., Sokabe, M., and Hasegawa, Y. (2009) Mechanical stretch enhances IL-8 production in pulmonary microvascular endothelial cells. *Biochem. Biophys. Res. Commun.* **389,** 531–536
25. Birukova, A. A., Moldobaeva, N., Xing, J., and Birukov, K. G. (2008) Magnitude-dependent effects of cyclic stretch on HGF- and VEGF-induced pulmonary endothelial remodeling and barrier regulation. *Am. J. Physiol. Lung Cell Mol. Physiol.* **295,** L612–L623
26. Shikata, Y., Rios, A., Kawkitinarong, K., DePaola, N., Garcia, J. G., and Birukov, K. G. (2005) Differential effects of shear stress and cyclic stretch on focal adhesion remodeling, site-specific FAK phosphorylation, and small GTPases in human lung endothelial cells. *Exp. Cell Res.* **304,** 40–49
27. Birukova, A. A., Tian, Y., Meliton, A., Leff, A., Wu, T., and Birukov, K. G. (2012) Stimulation of Rho signaling by pathologic mechanical stretch is a "second hit" to Rho-independent lung injury induced by IL-6. *Am. J. Physiol. Lung Cell Mol. Physiol.* **302,** L965–L975
28. Gawlak, G., Tian, Y., O'Donnell, J. J., 3rd, Tian, X., Birukova, A. A., and Birukov, K. G. (2014) Paxillin mediates stretch-induced Rho signaling and endothelial permeability via assembly of paxillin-p42/44MAPK-GEF-H1 complex. *FASEB J.* **28,** 3249–3260
29. Zimman, A., Mouillesseaux, K. P., Le, T., Gharavi, N. M., Ryvkin, A., Graeber, T. G., Chen, T. T., Watson, A. D., and Berliner, J. A. (2007) Vascular endothelial growth factor receptor 2 plays a role in the activation of aortic endothelial cells by oxidized phospholipids. *Arterioscler. Thromb. Vasc. Biol.* **27,** 332–338
30. Birukov, K. G., Bochkov, V. N., Birukova, A. A., Kawkitinarong, K., Rios, A., Leitner, A., Verin, A. D., Bokoch, G. M., Leitinger, N., and Garcia, J. G. (2004) Epoxycyclopentenone-containing oxidized phospholipids restore endothelial barrier function via Cdc42 and Rac. *Circ. Res.* **95,** 892–901
31. Birukova, A. A., Zebda, N., Cokic, I., Fu, P., Wu, T., Dubrovskyi, O., and Birukov, K. G. (2011) p190RhoGAP mediates protective effects of oxidized phospholipids in the models of ventilator-induced lung injury. *Exp. Cell Res.* **317,** 859–872
32. Birukov, K. G., Jacobson, J. R., Flores, A. A., Ye, S. Q., Birukova, A. A., Verin, A. D., and Garcia, J. G. (2003) Magnitude-dependent regulation of pulmonary endothelial cell barrier function by cyclic stretch. *Am. J. Physiol. Lung Cell Mol. Physiol.* **285,** L785–L797
33. Tschumperlin, D. J., Oswari, J., and Margulies, A. S. (2000) Deformation-induced injury of alveolar epithelial cells. Effect of frequency, duration, and amplitude. *Am. J. Respir. Crit. Care Med.* **162,** 357–362
34. Tschumperlin, D. J., and Margulies, S. S. (1999) Alveolar epithelial surface area-volume relationship in isolated rat lungs. *J. Appl. Physiol.* **86,** 2026–2033
35. Dubrovskyi, O., Birukova, A. A., and Birukov, K. G. (2013) Measurement of local permeability at subcellular level in cell models of agonist- and ventilator-induced lung injury. *Lab. Invest.* **93,** 254–263
36. Birukova, A. A., Fu, P., Xing, J., Yakubov, B., Cokic, I., and Birukov, K. G. (2010) Mechanotransduction by GEF-H1 as a novel mechanism of ventilator-induced vascular endothelial permeability. *Am. J. Physiol. Lung Cell Mol. Physiol.* **298,** L837–L848
37. Birukova, A. A., Birukov, K. G., Smurova, K., Adyshev, D., Kaibuchi, K., Alieva, I., Garcia, J. G., and Verin, A. D. (2004) Novel role of microtubules in thrombin-induced endothelial barrier dysfunction. *FASEB J.* **18,** 1879–1890
38. Birukova, A. A., Smurova, K., Birukov, K. G., Usatyuk, P., Liu, F., Kaibuchi, K., Ricks-Cord, A., Natarajan, V., Alieva, I., Garcia, J. G., and Verin, A. D. (2004) Microtubule disassembly induces cytoskeletal remodeling and lung vascular barrier dysfunction: role of Rho-dependent mechanisms. *J. Cell Physiol.* **201,** 55–70
39. Birukova, A. A., Malyukova, I., Mikaelyan, A., Fu, P., and Birukov, K. G. (2007) Tiam1 and betaPIX mediate Rac-dependent endothelial barrier protective response to oxidized phospholipids. *J. Cell Physiol.* **211,** 608–617
40. Birukova, A. A., Malyukova, I., Poroyko, V., and Birukov, K. G. (2007) Paxillin-β-catenin interactions are involved in Rac/Cdc42-mediated endothelial barrier-protective response to oxidized phospholipids. *Am. J. Physiol. Lung Cell Mol. Physiol.* **293,** L199–L211
41. Frank, J. A., and Matthay, M. A. (2003) Science review: mechanisms of ventilator-induced injury. *Crit. Care* **7,** 233–241
42. Birukova, A. A., Fu, P., Xing, J., Cokic, I., and Birukov, K. G. (2010) Lung endothelial barrier protection by iloprost in the 2-hit models of ventilator-induced lung injury (VILI) involves inhibition of Rho signaling. *Transl. Res.* **155,** 44–54
43. Dejana, E., Orsenigo, F., and Lampugnani, M. G. (2008) The role of adherens junctions and VE-cadherin in the control of vascular permeability. *J. Cell Sci.* **121,** 2115–2122
44. Orsenigo, F., Giampietro, C., Ferrari, A., Corada, M., Galaup, A., Sigismund, S., Ristagno, G., Maddaluno, L., Koh, G. Y., Franco, D., Kurtcuoglu, V., Poulikakos, D., Baluk, P., McDonald, D., Grazia Lampugnani, M., and Dejana, E. (2012) Phosphorylation of VE-cadherin is modulated by haemodynamic forces and contributes to the regulation of vascular permeability *in vivo*. *Nat. Commun.* **3,** 1208
45. Amado-Azevedo, J., Valent, E. T., and Van Nieuw Amerongen, G. P. (2014) Regulation of the endothelial barrier function: a filum granum of cellular forces, Rho-GTPase signaling and microenvironment. *Cell Tissue Res.* **355,** 557–576
46. Corada, M., Liao, F., Lindgren, M., Lampugnani, M. G., Breviario, F., Frank, R., Muller, W. A., Hicklin, D. J., Bohlen, P., and Dejana, E. (2001) Monoclonal antibodies directed to different regions of vascular endothelial cadherin extracellular domain affect adhesion and clustering of the protein and modulate endothelial permeability. *Blood* **97,** 1679–1684
47. Eggers, C. T., Schafer, J. C., Goldenring, J. R., and Taylor, S. S. (2009) D-AKAP2 interacts with Rab4 and Rab11 through its RGS domains and regulates transferrin receptor recycling. *J. Biol. Chem.* **284,** 32869–32880
48. Shay-Salit, A., Shushy, M., Wolfovitz, E., Yahav, H., Breviario, F., Dejana, E., and Resnick, N. (2002) VEGF receptor 2 and the adherens junction as a mechanical transducer in vascular endothelial cells. *Proc. Natl. Acad. Sci. U.S.A.* **99,** 9462–9467
49. Fujiwara, K. (2006) Platelet endothelial cell adhesion molecule-1 and mechanotransduction in vascular endothelial cells. *J. Intern. Med.* **259,** 373–380
50. Takai, Y., Ikeda, W., Ogita, H., and Rikitake, Y. (2008) The immunoglobulin-like cell adhesion molecule nectin and its associated protein afadin. *Annu. Rev. Cell Dev. Biol.* **24,** 309–342
51. Ooshio, T., Kobayashi, R., Ikeda, W., Miyata, M., Fukumoto, Y., Matsuzawa, N., Ogita, H., and Takai, Y. (2010) Involvement of the interaction of afadin with ZO-1 in the formation of tight junctions in Madin-Darby canine kidney cells. *J. Biol. Chem.* **285,** 5003–5012
52. Sun, H., Breslin, J. W., Zhu, J., Yuan, S. Y., and Wu, M. H. (2006) Rho and ROCK signaling in VEGF-induced microvascular endothelial hyperpermeability. *Microcirculation* **13,** 237–247
53. Beckers, C. M., van Hinsbergh, V. W., and van Nieuw Amerongen, G. P. (2010) Driving Rho GTPase activity in endothelial cells regulates barrier integrity. *Thromb. Haemost.* **103,** 40–55
54. Grazia Lampugnani, M., Zanetti, A., Corada, M., Takahashi, T., Balconi, G., Breviario, F., Orsenigo, F., Cattelino, A., Kemler, R., Daniel, T. O., and Dejana, E. (2003) Contact inhibition of VEGF-induced proliferation requires vascular endothelial cadherin, β-catenin, and the phosphatase DEP-1/CD148. *J. Cell Biol.* **161,** 793–804
55. Tzima, E., Del Pozo, M. A., Kiosses, W. B., Mohamed, S. A., Li, S., Chien, S., and Schwartz, M. A. (2002) Activation of Rac1 by shear stress in endothelial cells mediates both cytoskeletal reorganization and effects on gene expression. *EMBO J.* **21,** 6791–6800
56. Birukova, A. A., Rios, A., and Birukov, K. G. (2008) Long-term cyclic stretch controls pulmonary endothelial permeability at translational and post-translational levels. *Exp. Cell Res.* **314,** 3466–3477
57. Matsuzaki, I., Chatterjee, S., Debolt, K., Manevich, Y., Zhang, Q., and Fisher, A. B. (2005) Membrane depolarization and NADPH oxidase activation in aortic endothelium during ischemia reflect altered mechanotransduction. *Am. J. Physiol. Heart Circ. Physiol.* **288,** H336–H343

58. Sarelius, I. H., and Glading, A. J. (2015) Control of vascular permeability by adhesion molecules. *Tissue Barriers* **3,** e985954
59. Lambeng, N., Wallez, Y., Rampon, C., Cand, F., Christé, G., Gulino-Debrac, D., Vilgrain, I., and Huber, P. (2005) Vascular endothelial-cadherin tyrosine phosphorylation in angiogenic and quiescent adult tissues. *Circ. Res.* **96,** 384–391
60. Dejana, E. (2004) Endothelial cell-cell junctions: happy together. *Nat. Rev. Mol. Cell Biol.* **5,** 261–270
61. Privratsky, J. R., and Newman, P. J. (2014) PECAM-1: regulator of endothelial junctional integrity. *Cell Tissue Res.* **355,** 607–619
62. Conway, D., and Schwartz, M. A. (2012) Lessons from the endothelial junctional mechanosensory complex. *F1000 Biol. Reports* **4,** 1
63. Newman, P. J., and Newman, D. K. (2003) Signal transduction pathways mediated by PECAM-1: new roles for an old molecule in platelet and vascular cell biology. *Arterioscler. Thromb. Vasc. Biol.* **23,** 953–964
64. Chiu, Y. J., McBeath, E., and Fujiwara, K. (2008) Mechanotransduction in an extracted cell model: Fyn drives stretch- and flow-elicited PECAM-1 phosphorylation. *J. Cell Biol.* **182,** 753–763
65. Birukov, K. G., Birukova, A. A., Dudek, S. M., Verin, A. D., Crow, M. T., Zhan, X., DePaola, N., and Garcia, J. G. (2002) Shear stress-mediated cytoskeletal remodeling and cortactin translocation in pulmonary endothelial cells. *Am. J. Respir. Cell Mol. Biol.* **26,** 453–464
66. Peng, F., Zhang, B., Ingram, A. J., Gao, B., Zhang, Y., and Krepinsky, J. C. (2010) Mechanical stretch-induced RhoA activation is mediated by the RhoGEF Vav2 in mesangial cells. *Cell. Signal.* **22,** 34–40
67. Singh, A. J., Meyer, R. D., Band, H., and Rahimi, N. (2005) The carboxyl terminus of VEGFR-2 is required for PKC-mediated down-regulation. *Mol. Biol. Cell* **16,** 2106–2118
68. Birukova, A. A., Fu, P., Xing, J., and Birukov, K. G. (2009) Rap1 mediates protective effects of iloprost against ventilator induced lung injury. *J. Appl. Physiol.* **107,** 1900–1910
69. Birukova, A. A., Tian, X., Tian, Y., Higginbotham, K., and Birukov, K. G. (2013) Rap-afadin axis in control of Rho signaling and endothelial barrier recovery. *Mol. Biol. Cell* **24,** 2678–2688
70. Kooistra, M. R., Corada, M., Dejana, E., and Bos, J. L. (2005) Epac1 regulates integrity of endothelial cell junctions through VE-cadherin. *FEBS Lett.* **579,** 4966–4972
71. Cullere, X., Shaw, S. K., Andersson, L., Hirahashi, J., Luscinskas, F. W., and Mayadas, T. N. (2005) Regulation of vascular endothelial barrier function by Epac, a cAMP-activated exchange factor for Rap GTPase. *Blood* **105,** 1950–1955
72. Schlegel, N., and Waschke, J. (2014) cAMP with other signaling cues converges on Rac1 to stabilize the endothelial barrier: a signaling pathway compromised in inflammation. *Cell Tissue Res.* **355,** 587–596